Optical nonlinearity versus mechanical anharmonicity contrast in dynamic mode apertureless scanning near-field optical microscopy

Alpan Bek, Ralf Vogelgesang,[a] and Klaus Kern[b]
Max Planck Institut für Festkörperforschung, 70569 Stuttgart, Germany

(Received 26 April 2005; accepted 28 August 2005; published online 13 October 2005)

We show that the contrast mechanism in dynamic mode apertureless scanning near-field optical microscopy is in general a combination of both spatially nonlinear optical interaction and temporally anharmonic mechanical cantilever motion. Mechanical factors are found experimentally to easily overshadow the optical signal, leading to artifacts not yet well documented in the literature. Our algebraic analysis provides a systematic framework to identify and control the relative influence of the competing contrast origins. © *2005 American Institute of Physics*. [DOI: 10.1063/1.2108125]

Free-space optics using conventional far-field lens or mirror objectives for local excitation of light-matter interaction affords a spatial resolution which is limited by diffraction effects, typically to about half the wavelength, that is, a few 100 nm for visible radiation. Even though Synge[1] suggested already in 1928 to utilize optical near fields at a subdiffraction size aperture to go beyond this limit, only after 1970 was his idea realized.[2–6] By now, a great variety of aperture-based scanning near-field optical microscopy (SNOM) techniques has been established, yet the quest for ever-better resolution has recently introduced a novel type of nano-optical instrument. The scattering type or apertureless SNOM (aSNOM) has been demonstrated to offer local-field mapping[7–10] and also material contrast.[11–13]

The majority of aSNOM implementations so far are based on dynamic mode atomic force microscopes (AFMs), that is, the tip-sample distance is modulated periodically while an optical excitation field interacts with the tip-sample system. The strong nonlinear dependence of the scattered optical field on the tip-sample distance in the sub-10-nm range allows to extract near-field optical information at higher harmonics of the cantilever vibration frequency (Fig. 1). Here an essential assumption is that the local potential $U(d)$ of the cantilever motion is parabolic and its power spectrum $d(\omega)$ shows just a single peak at 1Ω (solid) with no anharmonic contributions (dashed). Ideally, $\mathcal{I}(\omega)$ contains purely near-field optical signals detectable at $2\Omega, 3\Omega, \ldots$, due to the nonlinearity of $\mathcal{I}(d)$; other optical interactions such as reflections or shadowing are suppressed as they vary linearly with the tip position and are detectable only at 1Ω. In general, however, the cantilever motion will always be somewhat anharmonic, leading to higher harmonics contributions to $\mathcal{I}(\omega)$ generated by the mechanical properties of the tip-sample system. Indeed, contrast in material surface properties can be obtained entirely nonoptically by deliberate excitation of anharmonic AFM cantilever motion and observation at higher harmonic frequencies.[14–21] In the context of dynamic mode aSNOM, this mechanical influence constitutes an important source of artifacts—hitherto underappreciated in the literature. For ideal measurements of optical contrast only, mechanical anharmonic contributions must be suppressed by careful choices of AFM drive and set point. Under suboptimal conditions, to recover the optical information, one needs additional measurements (varying mechanical or optical experimental parameters or tracing the cantilever motion separately) and an analytical model such as the one we develop in the following.

To analyze the essential features of the intricate interplay of mechanical anharmonicity and optical nonlinearity in dynamic aSNOM, we combine a Taylor and a Fourier expansion of the experimental signal. We do not consider directly the scattered radiation field $\mathbf{E}_s$ that carries the near-field optical information from the sample to a suitable detector. Instead, we focus on the electric photocurrent $\mathcal{I}$ generated in the detection process because different varieties of aSNOM setups may translate the optical into electric information quite differently. [For instance, $\mathcal{I} \propto |\mathbf{E}_s|^2$, $\mathbf{E}_s \cdot \overline{\mathbf{E}_r}$, and $\mathbf{E}_s \cdot \overline{\mathbf{E}_r} \exp(i\Omega_r t)$ for direct, homodyne, and heterodyne interferometric detection, respectively.] Common to all of them is that the photocurrent is modulated by the AFM tip oscillation $d(t)$ at an eigenfrequency $\Omega/2\pi \approx 50-500$ kHz. The $\mathcal{I}(d)$ dependence can be rather nonlinear for distances less than the effective radius of the tip apex (typically a few nanometers). A Taylor series expansion about a conveniently chosen reference distance d_r allows to keep only lowest-order terms,

$$\mathcal{I}(d) = \mathcal{I}^{(0)} + (d - d_r)\mathcal{I}^{(1)} + \tfrac{1}{2}(d - d_r)^2\mathcal{I}^{(2)} + \cdots .$$

Here, $\{\mathcal{I}^{(n)}\}$ are the real-valued nth derivatives of the scattered amplitude signal, which contain only *optical* information—about the tip-sample interaction and also the spatial behavior of the excitation field. Care must be taken in

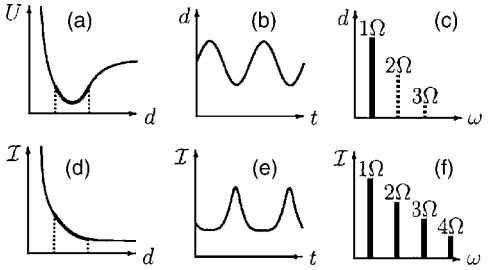

FIG. 1. Schematic of the dynamic aSNOM demodulation for true near-field optical contrast. (a) Effective potential U of the mechanical motion of the cantilever as a function of the tip-sample distance d. (b) Time behavior and (c) power spectrum of the cantilever motion. (d) The photocurrent $\mathcal{I}$ generated by the scattered radiation as a function of the tip-sample distance, its time behavior (e) and power spectrum (f).

[a]Electronic mail: r.vogelgesang@fkf.mpg.de
[b]URL: www.fkf.mpg.de/kern

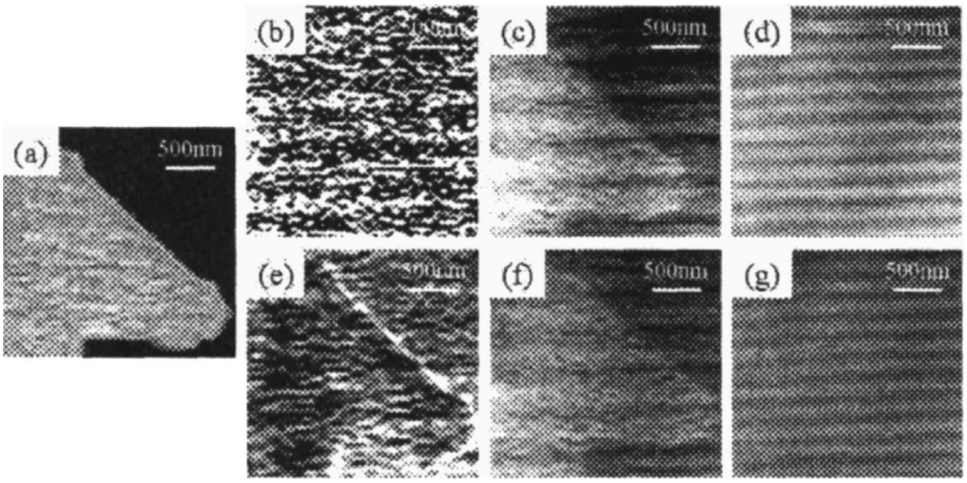

FIG. 2. An *e*-beam lithographically defined Au pattern on glass, recorded with a heterodyne interferometric aSNOM setup at $\lambda=633$ nm using a Au-coated Si cantilever. (a) Topography. (b)–(d) $\mathcal{S}_3^+$ for increasing drive voltage at cantilever oscillation amplitude setpoints of 9, 20, and 80 nm, respectively, keeping the set point to free-space amplitude ratio constant at ~96%. (e)–(g) $\mathcal{S}_3^+$ for increasing the drive voltage at a constant set point of 9 nm corresponding to 84%, 42%, and 21% of the free-space amplitudes, respectively.

choosing the reference location d_r. In the present context, as we discuss an oscillating tip, the average tip location d_0 is a natural choice, leading to low-order convergence. However, when the tip approaches the sample surface from afar or when the oscillation amplitude changes while in contact, the variable $d_0=d_r$ indirectly changes the coefficients $\mathcal{I}^{(n)}$ as well. Therefore, while in contact, an alternative choice is the fix, lower point of the tip oscillation $d_r=0$. In this case, we may consider variations in the oscillation amplitude and still the $\{\mathcal{I}^{(n)}\}$ remain constant.

In incorporating the time dependence of the AFM tip moving in a nonharmonic potential $U(d)$, an appropriate ansatz is the Fourier analysis into harmonics of the oscillation frequency Ω, where we expect only the lowest orders to be relevant. We chose the complex representation $d(t)=\Sigma_k d_k \exp(ik\Omega t)$, where the complex-valued coefficients fulfill $d_{-k}=d_k$ for real-valued $d(t)$. They contain strictly information about the *mechanical* properties of the tip-sample system. Notice that the average location d_0 of the tip and the amplitude of vibration $|d_1|$ are kept constant by the feedback loop of the AFM. The phase of d_1 reflects the lag between drive and tip oscillation. The anharmonic coefficients d_k for $k>1$ contain information about the total potential (with contributions from the tip-sample interaction potentials as well as the intracantilever potential associated with bending its beam) and require a detailed model and the solution of the corresponding differential equations of motion for any more specific interpretation.

The resulting complete expansion of the electrical signal generated by the optical detector,

$$\mathcal{I}(t)=\sum_k e^{ik\Omega t}\left[\mathcal{I}^{(0)}\delta_{0k}+\mathcal{I}^{(1)}d_k+\frac{1}{2}\mathcal{I}^{(2)}\sum_m d_{k-m}d_m+\frac{1}{6}\mathcal{I}^{(3)}\sum_{m,n} d_{k-m}d_{m-n}d_n+\cdots\right],$$

contains a mixture of optical and mechanical informations. (We absorb d_r in d_0 to ease the notation.) Evidently, there will be sidebands in the frequency domain at all integral multiples $k\Omega$ of the tip vibration frequency, which, with appropriate electronics to generate the corresponding electronic reference signals, can be recorded with a lock-in amplifier independently of each other.

The action of a two-phase lock-in amplifier can be represented in the complex domain by $(T\to\infty)$

$$\mathcal{S}_k^{\pm}=\frac{1}{T}\int_0^T \mathcal{I}[d(t)]e^{\pm ik\Omega t}dt.$$

Note that the identity relations $\overline{\mathcal{S}_k^+}=\mathcal{S}_k^-=\mathcal{S}_{-k}^+$ afford us with redundancy that compresses all obtainable information—optical and mechanical—into a reduced subset, say, $\{\mathcal{S}_{k\geq 0}^+\}$, of all complex coefficients. An actual dual-phase lock-in amplifier measures, of course, simultaneously the two real-valued quantities $\Re(\mathcal{S}_k^+)$ and $\Im(\mathcal{S}_k^+)$, from which the amplitude and phase of $\mathcal{S}_k^+$ can be determined.

One extreme case is the perfectly linear dependence of photocurrent and tip-sample distance for all $d(t)$,

$$\mathcal{S}_{k>0}^+=\mathcal{I}^{(1)}\overline{d_k}, \tag{1}$$

which yields purely mechanical information. This can be the case, for instance, if the excitation focus is misaligned not at the apex but at the bulk of the oscillating tip.

If the Fourier spectrum of the tip oscillation is perfectly harmonic, we have the opposite extreme case for obtaining purely optical information. In the leading order, the signal recorded at $k\Omega$,

$$\mathcal{S}_{k>0}^+=\frac{1}{k!}\mathcal{I}^{(k)}\overline{d_1}^k, \tag{2}$$

arises from the expansion coefficient $\mathcal{I}^{(k)}$. For aSNOM, we are interested in the nonlinear contributions generated by near-field optical tip-sample interactions at the tip's apex. Note that it is also possible to generate such signals solely with optical excitation fields that vary nonlinearly in space, which can be utilized to map eigenfields of nanometric structures.[22] Indeed, in the absence of any sample, the oscillating tip may be used to characterize the focus volume of the exciting radiation and to subsequently align the tip's apex with the exact center of the focus.

The undesired effect of intermixing anharmonic mechanical contributions with the nonlinear optical information in the measured signal arises when the tip-sample motion is excited beyond the perfectly harmonic motion ($d_k\neq 0$ for $k>1$). For example, when observing at 2Ω, there is in general a competition between $\mathcal{I}^{(1)}\overline{d_2}$ representing mechanical information, the term $\frac{1}{2}\mathcal{I}^{(2)}\overline{d_1}^2$ related with optical information, as well as the mixed term $\mathcal{I}^{(2)}d_0\overline{d_2}$.

As mentioned above, there are two main sources for undesired mechanical anharmonicities: When the cantilever is overdriven, the anharmonic beam-bending potential gives

rise to a sample-independent signal, setting an upper limit to the vibration amplitude. Second, the tip-sample interaction potential may be anharmonic due to, e.g., snap in, intermittent contact, or too low set point (i.e., the ratio of surface engaged to free-space cantilever oscillation amplitude). Snap in was found empirically to occur when the product of the spring constant and the vibration amplitude is less than $\sim$200 nN.[23] This implies a minimum amplitude for harmonic vibration of a given cantilever. If instead of the necessary true noncontact mode the AFM is operated in intermittent contact mode, many higher harmonics of the cantilever oscillation can be excited. An empirical rule of thumb,[24] which we verified by and large through independent checks (see below), ensures harmonic cantilever motion when the set point amplitude is kept above $\sim$90% of the free-space amplitude. It is imaginable that these upper and lower limits already contradict each other and prohibit the use of a given cantilever in aSNOM.

In Fig. 2 we illustrate effects of the competition between optical nonlinearity and mechanical anharmonicity with aSNOM studies of gold nanostructures on glass. For (b)–(d) we increased the drive voltage but kept the set point at $\sim$96% of the free-space amplitude, that is, $|d_1|$ grows proportionally. In (b) the signal is still below detectability, in (c) proper conditions for optical material contrast are met as predicted by Eq. (2), and in (d) the anharmonic cantilever potential gives rise to overwhelming contributions to terms involving $d_2, d_3, \ldots$. In the series [(b) and (e)–(g)] we again increase the free-space amplitude but keep the AFM feedback amplitude $|d_1|$ constant and thus decrease the set point to the free-space amplitude ratio. The dominant optical term of Eq. (2) remains below the detectability level as in (b) and any contrast that evolves is mechanical in origin. In (e) first signs of anharmonic motion are discernable at the topographical sample edges. In (f) we observe a nonoptical material contrast according to Eq. (1). Similarly to (d), in (g) sample-material- and topography-independent contrast due to anharmonic cantilever motion overwhelms the image. These findings underline the importance of avoiding mechanical contamination of the optical signal and call for independent checks of the optical image contrast mechanism.

Besides keeping the AFM vibration amplitude and set point in the limits already discussed, several approaches are possible to verify near-field optical contrast. As the desired optical information results from the tip-sample interaction only, *off-apex illumination* of the tip provides an effective means of identifying any remaining mechanical motion artifacts. In fact, the beam deflection signal used in the AFM feedback electronics is such a signal and testing for higher harmonics contributions to this signal may even be done simultaneously with optical data acquisition. Another essential check is the variation of the optical excitation properties, such as wavelength, polarization, or phase. Without alteration of the mechanical setup, any change in the image contrast obtained in this way will be due to the optical properties of the system.

In conclusion, we have shown that knowledge of the mechanical cantilever motion is crucial for true optical contrast in dynamic aSNOM. Experimental results demonstrate how contrast due to anharmonic motion may mimic or even eclipse nonlinear near-field optical contrast in a subtle way. The algebraic analysis of the relative influences we provide allows to identify and suppress undesired signal sources systematically.

[1] E. H. Synge, Philos. Mag. **6**, 356 (1928).
[2] J. Okeefe, J. Opt. Soc. Am. **46**, 359 (1956).
[3] E. A. Ash and G. Nicholls, Nature (London) **237**, 510 (1972).
[4] D. W. Pohl, W. Denk, and M. Lanz, Appl. Phys. Lett. **44**, 651 (1984).
[5] A. Lewis, M. Isaacson, A. Harootunian, and A. Muray, Ultramicroscopy **13**, 227 (1984).
[6] E. Betzig, J. K. Trautmann, T. D. Harris, J. S. Weiner, and R. L. Kostelak, Science **251**, 1468 (1991).
[7] F. Zenhausern, M. P. Oboyle, and H. K. Wickramasinghe, Appl. Phys. Lett. **65**, 1623 (1994).
[8] F. Zenhausern, Y. Martin, and H. K. Wickramasinghe, Science **269**, 1083 (1995).
[9] Y. Martin, F. Zenhausern, and H. K. Wickramasinghe, Appl. Phys. Lett. **68**, 2475 (1996).
[10] R. Hillenbrand and F. Keilmann, Phys. Rev. Lett. **85**, 3029 (2000).
[11] B. Knoll and F. Keilmann, Nature (London) **399**, 134 (1999).
[12] B. Knoll and F. Keilmann, Opt. Commun. **182**, 321 (2000).
[13] N. Ocelic and R. Hillenbrand, Nat. Mater. **9**, 606 (2004).
[14] M. Stark, R. Stark, W. Heckl, and R. Guckenberger, Appl. Phys. Lett. **76**, 3293 (2000).
[15] R. Hillenbrand, M. Stark, and R. Guckenberger, Appl. Phys. Lett. **76**, 3478 (2000).
[16] S. I. Lee, S. W. Howell, A. Raman, and R. Reifenberger, Phys. Rev. B **66**, 115409 (2002).
[17] R. Garcia and R. Perez, Surf. Sci. Rep. **47**, 197 (2002).
[18] S. Lee, S. Howell, A. Raman, and R. Reifenberger, Ultramicroscopy **97**, 185 (2003).
[19] R. W. Stark and W. M. Heckl, Rev. Sci. Instrum. **74**, 5111 (2003).
[20] R. W. Stark, Nanotechnology **15**, 347 (2004).
[21] T. R. Rodriguez and R. Garcia, Appl. Phys. Lett. **84**, 449 (2004).
[22] R. Hillenbrand, F. Keilmann, P. Hanarp, D. S. Sutherland, and J. Aizpurua, Appl. Phys. Lett. **83**, 368 (2003).
[23] F. J. Giessibl, Habilitation thesis, Universität Augsburg, 2000.
[24] R. Hillenbrand, Ph.D. thesis, Technische Universität München, 2001.